Materials and Methods

Yeast Strains and Culturing Conditions

Saccharomyces cerevisiae strain culturing and transformations were performed using standard techniques. BY4741 (MAT a) was the background strain for all strains constructed and used, except for growth assays on SC (synthetic complete) -CYS-MET media, in which BY4742 (MAT α) was used as the background strain due to auxotrophies (1). *SIR4* was deleted from all strains to make all strains amenable to the calling card assay protocol, unless otherwise noted. Because *MET4* deletion results in a severe growth defect on YPD media, *OPI1* was first deleted in the *cbf1Δ met4Δ* strain to recreate a *met4Δ* suppressor mutant background (2). A complete catalogue of all strains constructed and used in this study is given in *SI Appendix,* **Supplemental Table 4**.

SC plates were composed of 20 g glucose (Acros Organics Cat No. 410950050), 1.7 g Yeast Nitrogen Base (BD Difco Cat. No. 233520), 2 g drop-out mix (BD Difco or Sunrise Science Products), per liter 5 g ammonium sulfate (Sigma-Aldrich Cat. No. A4915). Drop-out mixes were obtained from US Biological, except for SC-CYS-MET (Sunrise Science Products Cat. No. 1319).

To construct strains in which TF binding sites were mutated in specific promoter regions, the URA flip-out method was used (3). Strains with 100 – 300bp of DNA replaced by the URA3 gene cassette were transformed with PCR-amplified gBlocks® Gene Fragments (Integrated DNA Technologies) with the desired mutations. Sequences of mutated genomic promoters are given in *SI Appendix*, **Fig. S8**.

Plasmid Construction and Design

Plasmids were constructed using gap-repair yeast cloning and standard protocols (4). Wild-type and truncated TFs were expressed from the *ADH1* promoter and C-terminally tagged with the C-terminal domain of Sir4p (and 3X MYC tag) recognized in the calling card assay (5, 6), unless otherwise noted. (Strains presented in Fig 2E, Fig 3B, and Fig 6B do *not* express factors tagged with Sir4p.) Constructs expressing chimeric TFs were created by gap-repair cloning using PCR-amplified DNA from GeneArt® Gene Synthesis (Invitrogen). Truncated TFs were additionally tagged at the N-terminus with a 24 amino acid nuclear localization signal: MDKAELIPEPPKKKRKVELGTALQ. Basic, helix 1, loop, helix 2, and leucine-repeat Zipper of bHLH TFs were assigned using the Clustal Omega alignment tool (7) (RRID: SCR_001591). An additional 8-12 amino acids immediately N-terminal to the annotated basic sub-region was also retained in the truncated factors to help ensure proper secondary structural folding of the factor. The DNA-binding domain subregions of bHLH TFs were annotated as follows: Cbf1p R223-R234 (basic), R235-L249 (helix 1), P250-S255 (loop), K256-L270 (helix 2), K271-A351 (Zip); Tye7p Q181-Y192 (basic), R193-I207 (helix 1), P208-N250 (loop), K251-L265 (helix 2); NPAS2 K10-R21 (basic), R22-L36 (helix 1), P37-D44 (loop), K45-H59 (helix 2). In addition, the remaining 26 amino acids C-terminal to the helix 2 were included as part of the Tye7p DBD; 19 amino acids immediately C-terminal to the helix 2 were included as part of the Cbf1p bHLH construct; and 18 amino acids immediately C-terminal to the helix 2 were included in the NPAS2 bHLH. Where indicated, TFs were tagged with Met4p at the C-terminus with a 12 amino acid peptide linker sequence GGGSPAVSGGPS.

Yeast Calling Card Assay

The yeast calling card assay was performed essentially as previously described (5, 6, 8). Yeast strains were co-transformed with two centromeric yeast shuttle vectors (*LEU2* and *URA3* auxotrophic markers, respectively), one expressing the SIR4p-tagged TF from the *ADH1* promoter (unless indicated otherwise) and one expressing the *GAL1/10* promoter-regulated Ty5 retrotransposon carrying the *HIS3* auxotrophic marker. An overnight culture in SC with auxotrophic selection was then spread onto 4 – 7 SC with auxotrophic selection agar plates supplemented with galactose (Sigma-Aldrich Cat. No. G0750) as the carbon source and allowed to incubate at room temperature for 3 days. Plates were then sequentially replica-plated to YPD (2 day incubation 30°), SC-HIS supplemented with 5-FOA (3 day incubation 30°), and again to SC-HIS supplemented with 5-FOA agar plates

(2 day incubation 30°). Growth on SC-HIS supplemented with 5-FOA was performed to select for Ty5 integration events and counter-select the presence of the Ty5 centromeric plasmid. Cells were then harvested, pooled together, and genomic DNA was prepared using standard protocols. Genomic DNA from each assay was then digested in three separate digest reactions by HpaII (NEB Cat. No. R0171), HinP1I (NEB Cat. No. R0124), and Taq$^{\alpha}$1 (NEB Cat. No. R0149), purified (QIAquick PCR Purification Kit Qiagen Cat. No. 28106), and ~600 ng digested DNA was then self-ligated using T4 DNA Ligase (NEB Cat. No. M0202) according to manufacturer's protocols. Self-ligated genomic DNA was then purified (Amicon Ultra – 0.5 mL Centrifugal Filters Merck Millipore Cat. No. UFC503096) and used as template in an inverse PCR reaction. PCR primers used were designed to amplify the genomic DNA from the self-ligated template and had P5 and P7 Illumina sequencing platform adapters. Because experiments analyzing more than one TF were not pooled until after PCR, the forward primer for each calling card assay contained a 5 bp experiment barcode. Purified PCR products were then pooled in equimolar concentrations and submitted for next-gen Illumina sequencing.

Paired-end Sequence Map Back to Identify Ty5 Insertion Sites

DNA sequencing reads were filtered on two criteria: Read 1 sequences must have the correct 17 bp Ty5 3'LTR sequence, and the experiment-specific barcodes on both Read 1 (5 bp) and Read 2 (8 bp) must match. Following filtering of the reads, 80 bp of Read 1 genomic sequence was aligned to the *Saccharomyces cerevisiae* reference genome sacCer2 (R-61-1-1) after the 17bp LTR and Read1 barcodes were removed from the 5' end. Alignment was performed using NovoAlign with default parameter settings (www.novocraft.com) (RRID: SCR_014818).

Identification of Target Intergenic (Promoter) Regions

Promoters were defined as all intergenic regions spanning 150 bp into the ORF of the upstream and downstream gene that were smaller than 5kb in length. To quantitate TF binding to a given intergenic (promoter) region and account for differing numbers of total insertions per experiment, we normalized the number of Ty5 insertions into each intergenic region such that the total number of insertions recovered for each experiment was equal to 100,000 and assigned a Transposons per Hundred Thousand (TPH) value to the TF binding at each intergenic region. P-values measuring the statistical significance of binding were calculated by first calculating the expected number of insertions at each intergenic region under the null from the "No TF" negative control sample, which measures the rate of random Ty5 insertion into the genome. Poisson statistics were used then used to calculate the p-value from these null distributions. For statistical comparisons across different experimental samples, background subtracted TPH scores (STPH) were used. These were computed by subtracting the TPH values of the "No TF" negative control samples from the experimental samples. Binding target intergenic (promoter) regions were defined as those having a p-value <1e-5.

Western Blotting

O/N cultures were back diluted into 50 mL SC broth to a final concentration of 0.1 OD 660. The subculture was grown for ~5 hours and then harvested. Cells were washed in 500 uL protein extraction buffer (1.5M Tris-HCl pH 6.8, 0.6% SDS, 15% Glycerol). Cells were then resuspended in 150 uL of protein extraction buffer. 30 uL of glass microbeads were added, followed by vortexing at max speed for 20 minutes. The disrupted cells were pelleted at max speed for 10 minutes at 4°, and the supernatant was separated on a 12% polyacrylamide gel, followed by transfer to PVDF membrane. Twofold serial dilutions of each sample were analyzed with a myc-tagged protein standard to quantify protein abundance (Recombinant Posi-Tag Epitope Tag Protein, BioLegend). After blocking with 5% nonfat milk for 1 hr at room temperature and three washes with PBS + tween 0.02%, the membrane was incubated with primary antibody O/N at 4°. 1:1000 c-Myc (9E10):SC-40 (Santa Cruz) was used for our protein of interest, and 1:1000 Actin Monoclonal Antibody (mAbGEa) (Invitrogen) was used as loading control. After three washes, the membrane was incubated with 1:2000 mouse IgG kappa binding protein conjugated to HRP (Santa Cruz) for 1 hr at room temperature. After three more washes with PBS + 0.02% Tween, chemiluminescent imaging was performed using WesternBright substrate (Advansta).

ß-Galactosidase Reporter Assays

The *sir4Δ* and *sir4Δ gcr2Δ* strains were transformed with plasmid expressing ß -Galactosidase from the *TEF1* promoter. Following overnight culture in SC-LEU liquid media, cells were back-diluted 1:100 into SC-LEU with galactose, to mimic calling card induction conditions, and further incubated with shaking for 5 hrs. ß-Galactosidase assay was conducted using Yeast ß -Galactosidase Assay Kit (Thermo Scientific Prod #75768) according to "Microcentrifuge Tube Protocol" in manufacturer's instructions.

Position Specific Weight Matrices (PWMs)

For all analyses involving yeast TF PWMs, the matrices used were those recommended by Spivak and Stormo (9) and obtained from the ScerTF database (http://stormo.wustl.edu/ScerTF/) (RRID: SCR_006121). In all instances, scoring cutoffs used were those recommended by ScerTF, except for the Tye7 collective binding analysis present in Fig 4D, where "weak" sites were identified with a cut-off that was 2 units below the recommended threshold, but "normal" Tye7p/Gcr1p/Rap1p were identified with the recommended cutoffs. The NPAS2 PWM was obtained from the database of motifs used in the HOMER analysis package (10).

Receiver Operator Curves (ROC)

Receiver operator curves plot true positive rate (TPR) vs. false positive rate (FPR), with a perfect classifier yielding an area under the curve (AUC) of 1.0. For Tye7p and Cbf1p binding target ROC curves, "true positives" were defined as statistically significant binding measured by calling card assay, while "false positives" were defined as loci that did not display statistically significant binding. The scoring function used to classify Cbf1p and Tye7p targets was the highest scoring motif in a given intergenic promoter region. The Tye7p collective classifier used in Fig 4B is the sum of the highest scoring PWM motif scores for Gcr1p, Rap1p, and Tye7p within a 150 bp window of a given intergenic promoter region. For the histogram of AUCs shown in **Fig. 5*D***, true positive and false positive lists were defined using previously published ChIP-chip data (11). Motifs were identified and AUCs were computed using code written in Python that used the MOODS package (12, 13).

Cbf1p vs Tye7p Binding Target Prediction Decision Tree

Predicted Cbf1p binding targets include intergenic (promoter) regions meeting at least one of the following criteria: one Cbf1p motif meeting the recommended PWM score cut-off with no Rap1p or Gcr1p motifs nearby (within 150 bp) or at least two Cbf1p motifs within 500 bp. These window sizes were chosen because we observed strong homotypic cooperativity between Cbf1p homodimers bound within 500 bp (**Fig. 3*D***), and we observed that at least two Tye7p "collective" motifs occurred within 150bp at all Tye7p bound promoters (see Results). Predicted Tye7p binding targets include intergenic (promoter) regions displaying a motif at the recommended PWM score cut-off for at least two of three Tye7p collective members: Tye7p, Gcr1p, or Rap1p, within a 150 bp window distance. An intergenic (promoter) region with two separate sequence windows meeting both Cbf1p and Tye7p binding target requirements are classified as bound by both TFs.

Further Bioinformatic Analysis

Calling Card and ChIP data were compared to previously published mRNA expression data from *cbf1Δ* or *tye7Δ* knockout strains (Hu et al., 2007) in **Fig. 1*B*** by replicating a previously published analysis comparing the Hu and Harbison datasets (14). Briefly, differentially expressed genes were identified using the same statistical thresholds as Hu *et al*. The significance of overlap between Calling Card (or ChIP) data and these data was calculated from the cumulative hypergeometric distribution. To ensure that our conclusions were robust to the particular statistical cutoffs used for the Calling Card or ChIP data, this analysis was performed over a range of cutoffs for both Calling Card and ChIP and plotted. For **Fig. 4*B***, the significance threshold we used to overlap the Rap1p Chec-Seq data with calling card binding data was that used in the original publication (15).

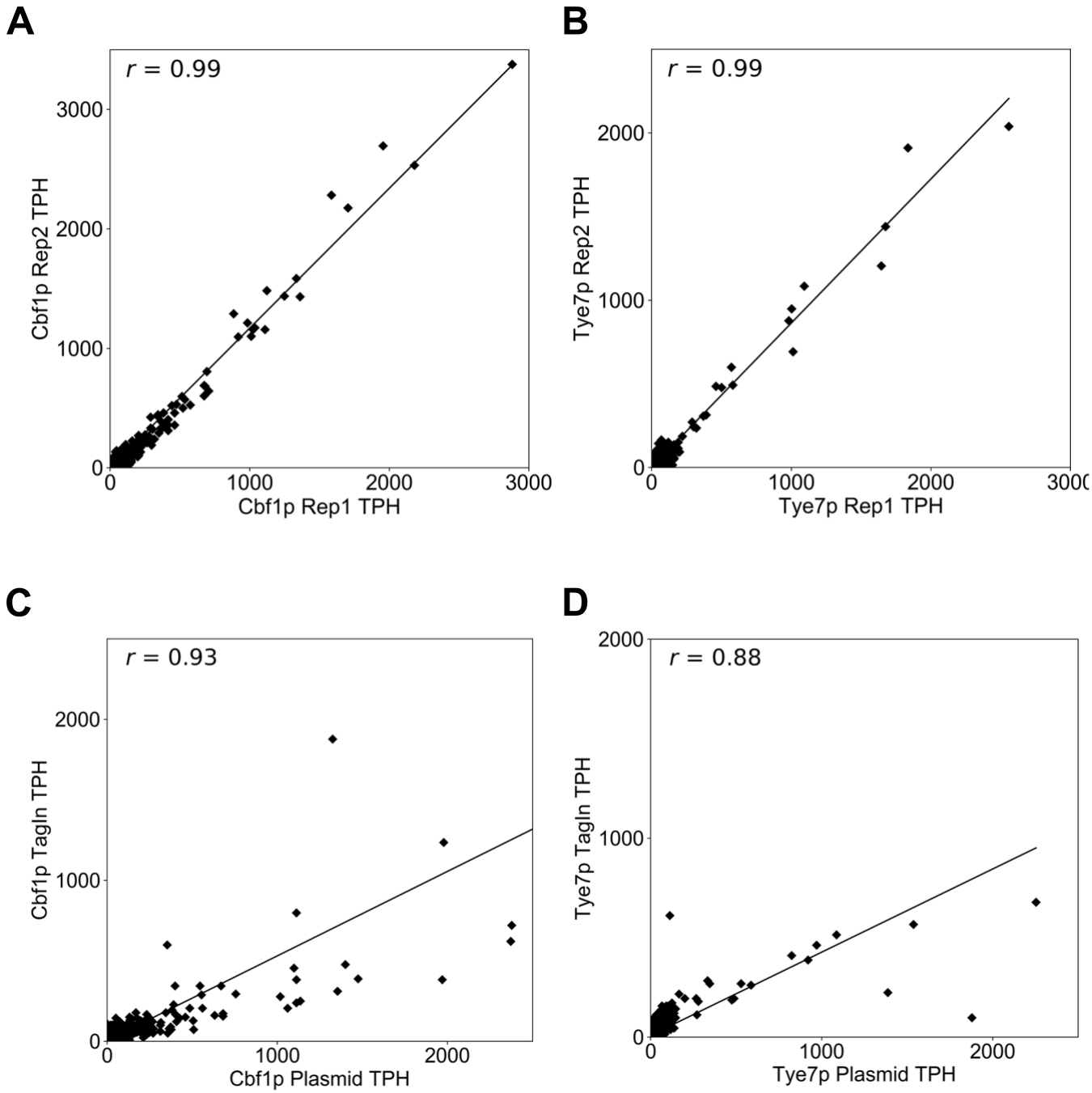

Fig. S1. A. Reproducibility of Cbf1p binding pattern assayed by calling cards. The genome-wide intergenic binding (TPH) of two Cbf1p replicates (Rep1 and Rep2) is plotted, with each point representing a single intergenic region. B. Reproducibility of Tye7p binding pattern assayed by calling cards. The genome-wide intergenic binding (TPH) of two Tye7p replicates (Rep1 and Rep2) is plotted, with each point representing a single intergenic region. C. The binding patterns of Cbf1p expressed from plasmid or endogenous locus are highly concordant. The genome-wide intergenic binding (TPH) of Cbf1p expressed from plasmid (x-axis) vs. endogenous locus (y-axis "tagin") is plotted, with each point representing a single intergenic region. D. The binding patterns of Tye7p expressed from plasmid or endogenous locus are highly concordant. The genome-wide intergenic binding (TPH) of Tye7p expressed from plasmid (x-axis) vs. endogenous locus (y-axis "tagin") is plotted, with each point representing a single intergenic region.

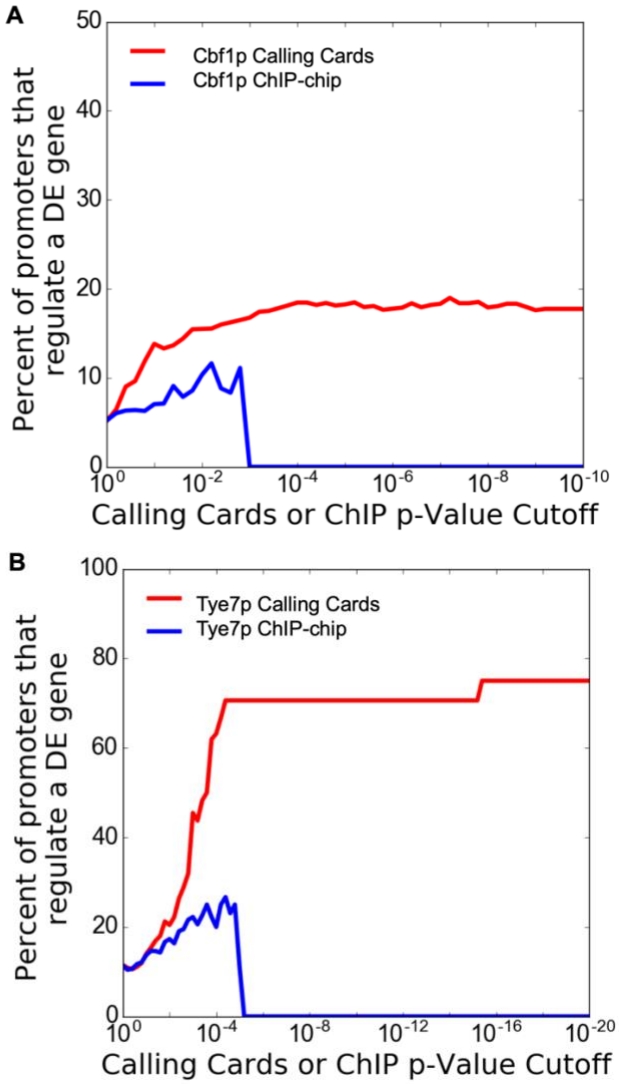

Fig. S2. Percent responsive genes bound by Cbf1p and Tye7p as measured by calling card assay or ChIP-chip (Harbison et al., 2004). The x axis of each graph in A – C indicates the p-value cut-off for significantly bound targets for each assay. The percentage of bound promoters found to be differentially expressed (DE) is plotted on the y-axis. The DE gene set used was obtained by mRNA expression profiling of *cbf1Δ* (A) or *tye7Δ* (B) deletion strains (Hu et al., 2007). For Cbf1p, the fraction bound curves for calling card and chip are somewhat nearer to one another than the hypergeometric pvalue curves observed in Fig 1B because at a given cutoff, there are many more calling card targets than ChIP targets, accounting for the difference in significance. A similar analysis that performs a comprehensive comparison of calling card data with TF perturbation data has recently been published. (16)

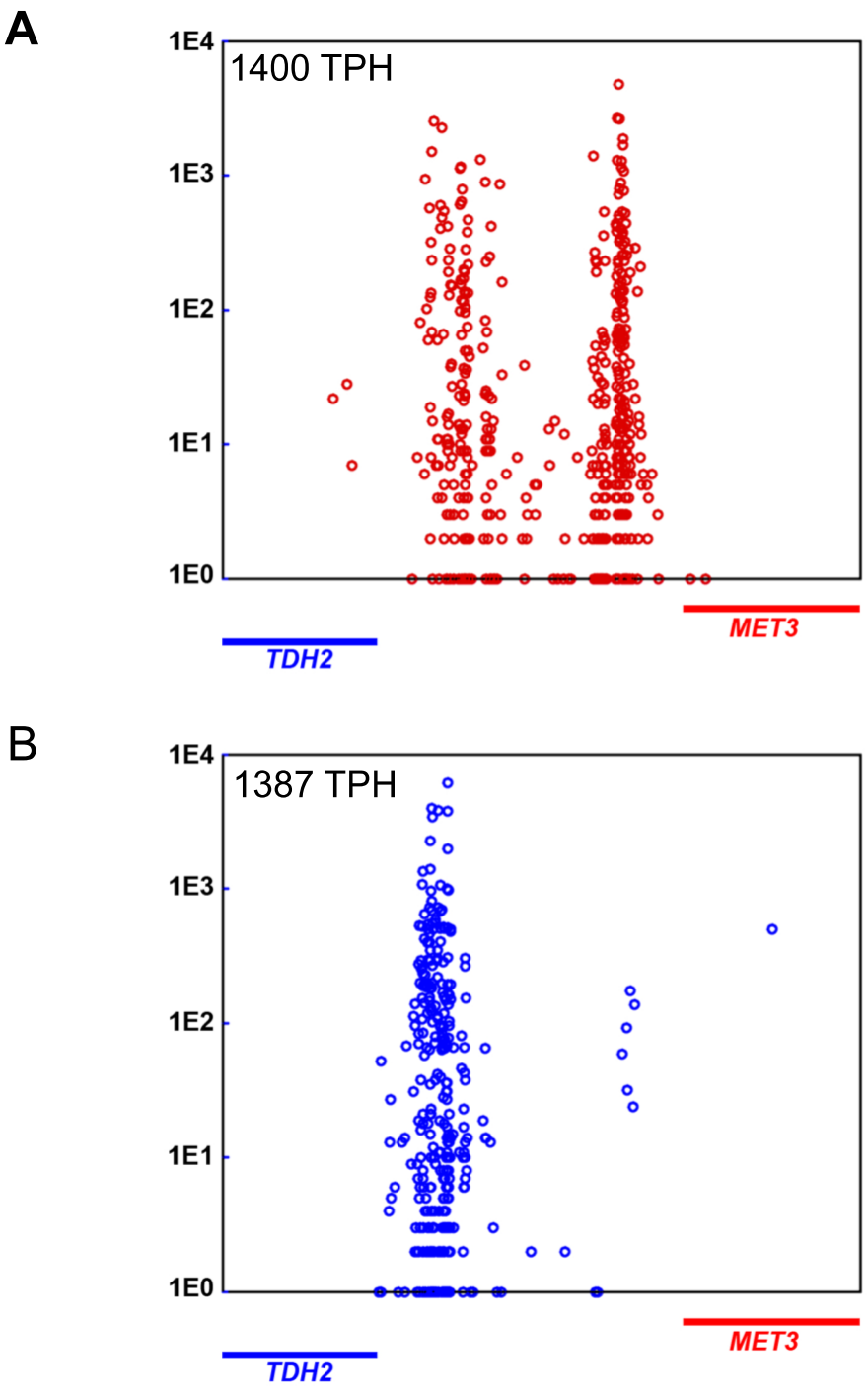

Fig. S3. Binding of Cbf1p and Tye7p to the divergent promoter of *TDH2* and *MET3*. Cbf1p-directed calling card insertions are indicated by red circles (A), while Tye7p insertions are indicated by blue circles (B).

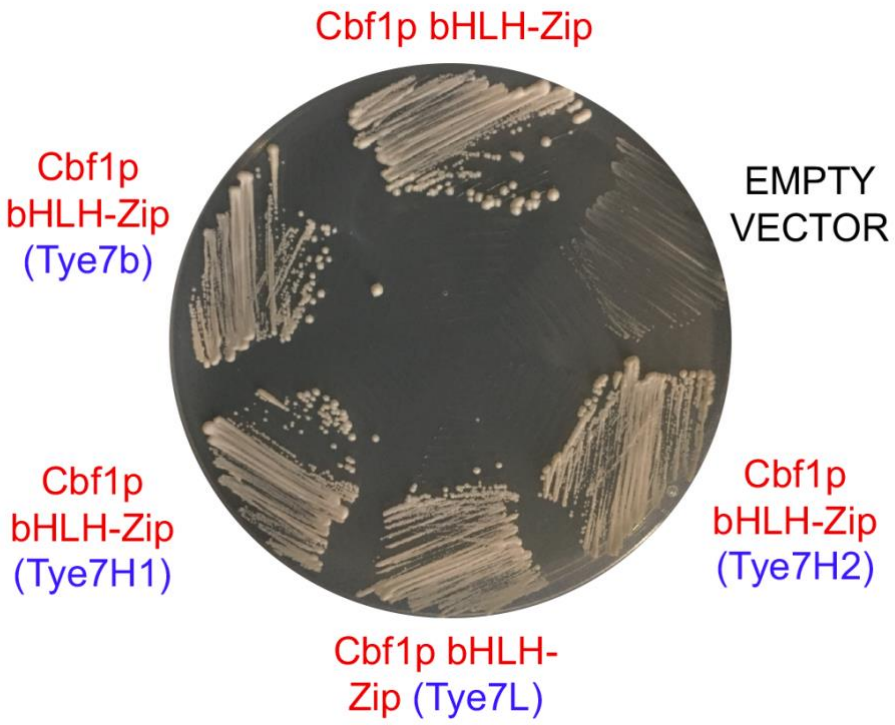

Fig. S4. Cbf1p bHLH-Zip chimera with a c-terminal Sir4p tag. To confirm that Cbf1 bHLH-Zip chimeras with Sir4p tags are still functional, we tested these constructs for functional rescue of a *cbf1Δ* strain on MET/CYS deficient media. (Parallel experiment to **Fig. 3*E***, but these proteins have Sir4p tags). These results demonstrate that all of these chimeras are still functional, and so the calling card data likely reflects native binding.

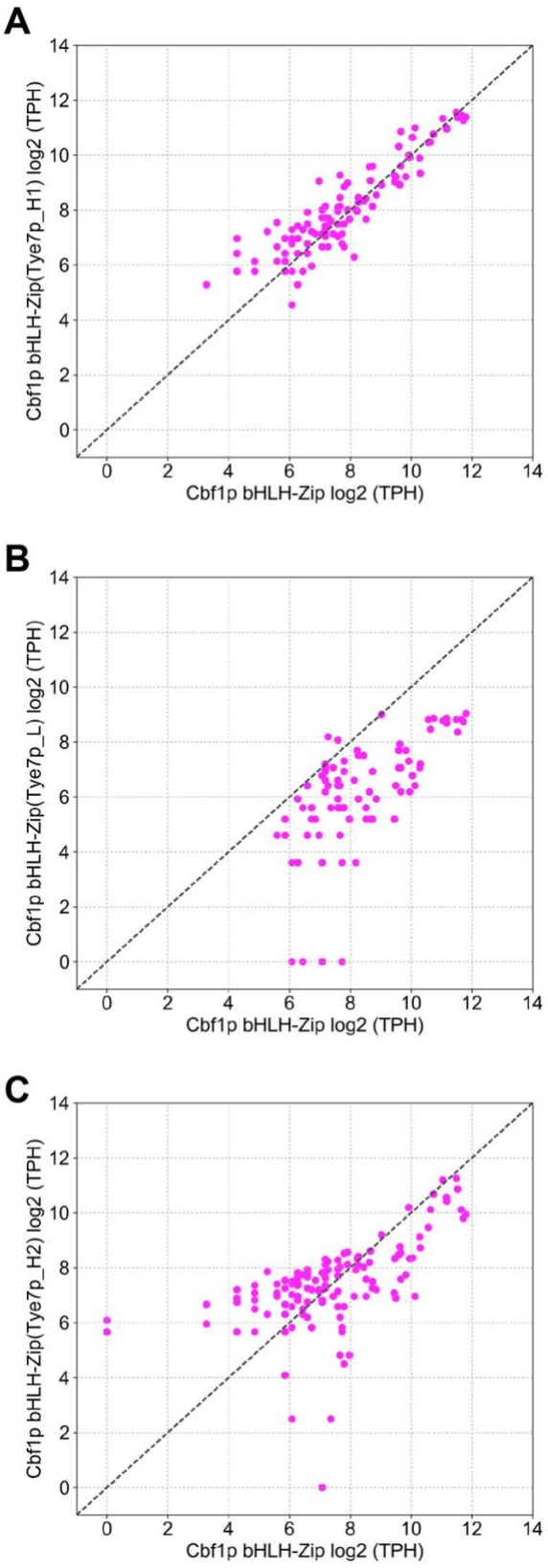

Fig. S5. The genomic binding patterns of Cbf1p bHLH-Zip chimera are similar to wild-type Cbf1p bHLH-Zip. The genome-wide intergenic binding (TPH) of Cbf1p bHLH-Zip(Tye7p_H1) (A), Cbf1p bHLH-Zip(Tye7p_L) (B), and Cbf1p bHLH-Zip(Tye7p_H2) (C) vs. wild-type Cbf1p bHLH-Zip to targets significantly bound by either factor are plotted, with each point representing a single intergenic region.

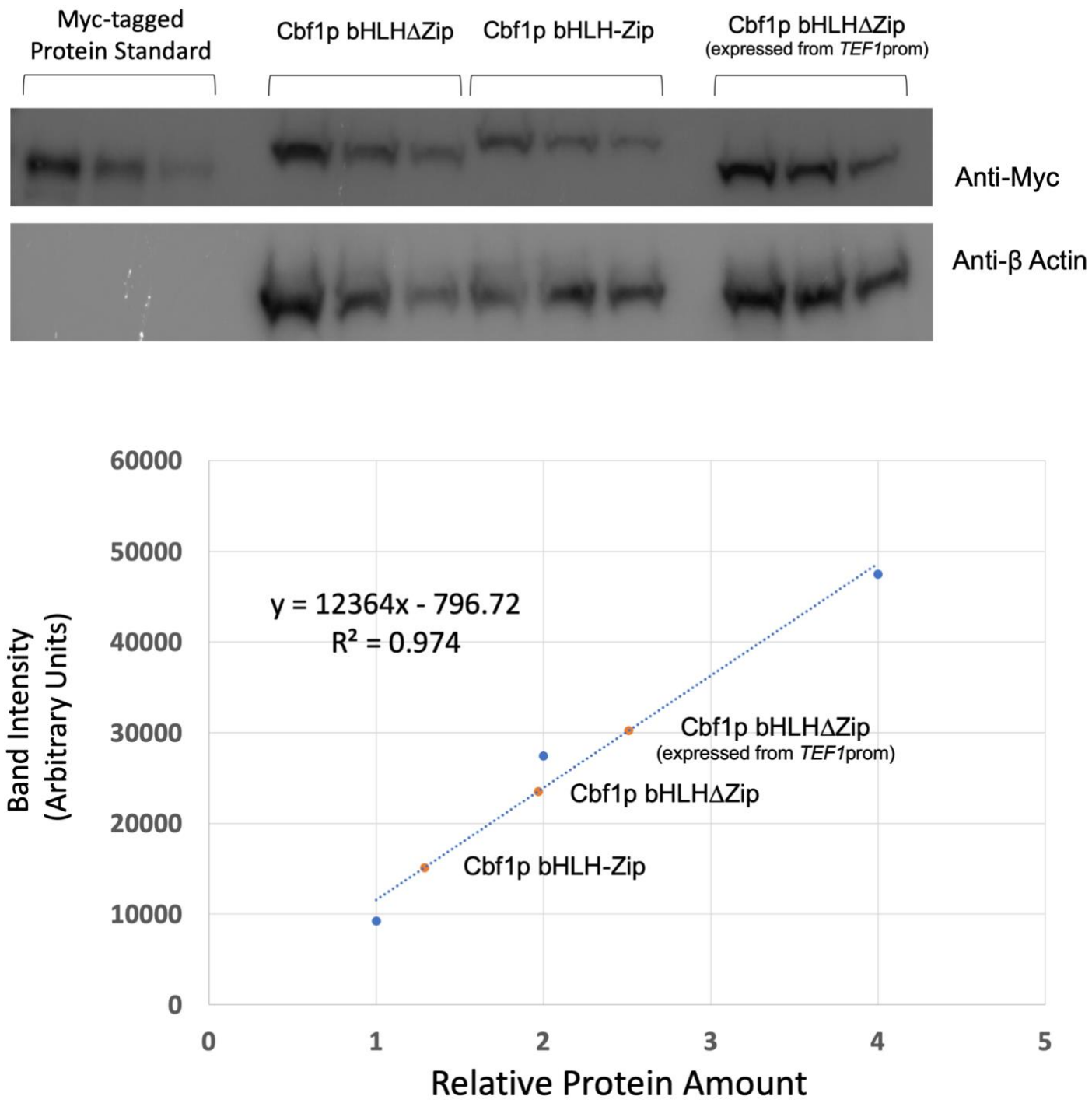

Fig. S6. Cbf1p bHLHΔZip (expressed from either the *ADH1* promoter or *TEF1* promoter) is slightly more highly expressed than Cbf1p bHLH-Zip (expressed from *ADH1* promoter) in the *cbf1Δ* strain, and so high levels of Cbf1p bHLH-Zip cannot explain the excess binding observed. A semi-quantitative Western blot was performed using serial dilutions of a MYC-tagged standard protein, Cbf1p bHLH-Zip (expressed from the *ADH1* promoter), Cbf1p bHLHΔZip (expressed from the *ADH1* promoter), and Cbf1p bHLHΔZIP (expressed from the *TEF1* promoter). TFs were probed with antibody to the MYC tag, c-terminal to the Sir4p tag, and probe against β-actin is shown as loading control (top). A standard curve was created using densitometry of the MYC-tagged protein standard bands (blue points on the graph), and relative amounts of each factor were interpolated (orange points on the graph), using the β-actin-normalized band intensities from the middle dilution for each factor (bottom).

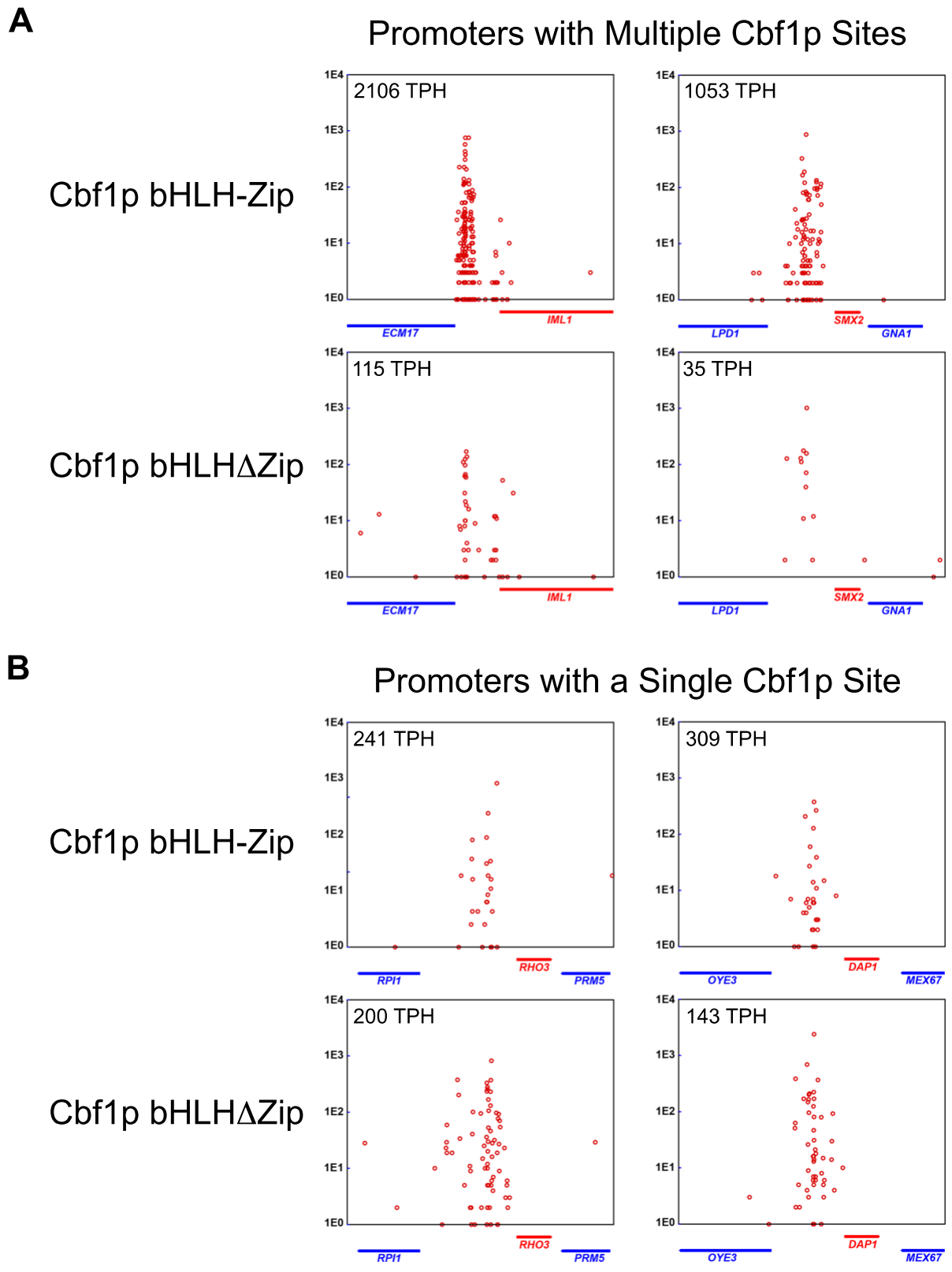

Fig. S7. Cbf1 bHLH-Zip and Cbf1 bHLHΔZip bind to the same sites in the genome; however, binding of Cbf1p bHLH-Zip is stronger (as measured by TPH) to targets possessing more than one Cbf1p motif at the recommended PWM cut-off (top) vs. targets with a single Cbf1p motif (bottom).

Fig. S8. Sequences of mutated promoters (intergenic regions) in the genome.

A. The mutated *IDH1* promoter. All possible permutations of 1, 2, or all 3 mutated Cbf1p site motifs were created; however, for brevity, only the IDH1 promoter with all three Cbf1p motif sites mutated is shown below. 1,000 bp of sequence upstream of the start ATG are displayed, and Cbf1p site motifs are shown in red, with mutated residues in lowercase.

GTTGTAACGCGAATCGGAGCAGCCGATGAAAAGAGTGTGAGGGGACTGGCCCTTCGCATTGTGATCTGGGAACAAAGTTGGCTGTATGTTGTTCATCTGGGAGGC
CCATTTGGCATTGGCGGCCAAGATATCTTGTAGGTTTGAGTTGTGACTCAATGTGAATATAGATGAAGATTCGGTAGCGCTCATTCTGATGTGTAATAATTGAAATTT
GTAGTCTTAGCTGTAGTTGATGTGGTTGGGGTTTTCAGAAGAAAACGAACAAGAATTAGAAGAGGACAGCTCTTACCTATCCTCGAGAATCATTACTTCCTAAGTAT
TTATAGTACTCTATGTCAGCCTACTTGTTCATTTCAAAATTACTCATCGAGAGAGGGGGAGGAAGGAATCACTAGTAATTTTTTCGGCTTGATAAGCGTCATGGTGAC
AATGCGAATTAATTCAGTGGCGTCAAGTTAGCTCATTCTGACGTCAACATCGAAACGGGAACGAACGTTCGTGCGGGGTGATGGTTAGAAAGtACGatACTTACGTT
ACTATtcaGTGATAACAATCACACTGTACGGCTGATCAAATTTTTTTCGGCGCCGAGTTTAGGTGAATCACtgaTGCCTGACCACCTTCTCCGAGCATCGGGCGTCATA
GGTCACTCATCAACCAACCATATTGCAGAAACCTTCTTTTATTTTTTTTGGTAGCTCGGTATTGTTATTTAGCGATTAAAGGAAGACCCTCATATATATATCCCCGTACA
ATACATGCCTACACTGAATATATATATAAGTGTTTTATGTGGGTGAGCACATAGGACTATCTATATTTTCCATAGGTCTTTTTTCTTGTTTTCTTCCGCTTCATTGGCTTA
TTCTTGATTGATTGATTTCTTTACTCTACCGTAGATCTATTTCAACAGTACCTTAATATTACTGGTAACAATCAAGGTTCATTATTCTCCCTATCCTCATTCTTCTCCCTTT
TCCTCCATAATTGTAAGAGAAAAATG

B. The mutated *TDH3* promoter sequence. 1000 bp of sequence upstream of the start ATG of the *TDH3* gene is shown with Gcr1/2p binding sites in blue and Rap1p binding sites in green. Lowercase indicates mutated bases.

CTATTTTCGAGGACCTTGTCACCTTGAGCCCAAGAGAGCCAAGATTTAAATTTTCCTATGACTTGATGCAAATTCCCAAAGCTAATAACATGCAAGACACGTACGGTC
AAGAAGACATATTTGACCTCTTAACAGGTTCAGACGCGACTGCCTCATCAGTAAGACCCGTTGAAAAGAACTTACCTGAAAAAAACGAATATATACTAGCGTTGAAT
GTTAGCGTCAACAACAAGAAGTTTAATGACGCGGAGGCCAAGGCAAAAAGATTCCTTGATTACGTAAGGGAGTTAGAATCATTTTGAATAAAAAACACGCTTTTTCA
GTTCGAGTTTATCATTATCAATACTGCCATTTCAAAGAATACGTAAATAATTAATAGTAGTGATTTTCCTAACTTTATTTAGTCAAAAAATTAGCCTTTTAATTCTGCTG
TAACttGTAaATaCCCAAAATAGGGGGCGGGTTACACAGAATATATAACATCGTAGGTaTCTaaGTGAACAGTTTATTCCTtGCAaCgACTAAATATAATGGAGCCCGC
TTTTTAAGCTGtCATtCAGAAAAAAAAAGAATCCCAGCACCAAAATATTGTTTTCTTCACCAACCATCAGTTCATAGGTCCATTCTCTTAGCGCAACTACAGAGAACAG
GGGCACAAACAGGCAAAAAACGGGCACAACCTCAATGGAGTGATGCAACCTGCCTGGAGTAAATGATGACACAAGGCAATTGACCCACGCATGTATCTATCTCATT
TTCTTACACCTTCTATTACCTTCTGCTCTCTCTGATTTGGAAAAAGCTGAAAAAAAAGGTTGAAACCAGTTCCCTGAAATTATTCCCCTACTTGACTAATAAGTATATAA
AGACGGTAGGTATTGATTGTAATTCTGTAAATCTATTTCTTAAACTTCTTAAATTCTACTTTTATAGTTAGTCTTTTTTTTAGTTTTAAAACACCAAGAACTTAGTTTCGA
ATAAACACACATAAACAAACAAAATG

C. The "reprogrammed" *TDH3* promoter sequence. 1,000 bp of sequence upstream of
the start ATG of the *TDH3* gene is shown with Gcr1/2p binding sites in blue and Rap1p binding sites in green. Lowercase indicates mutated bases. Sequence in red indicates that native sequence was mutated to Cbf1p binding sites as found in the *IDH1* promoter.

CTATTTTCGAGGACCTTGTCACCTTGAGCCCAAGAGAGCCAAGATTTAAATTTTCCTATGACTTGATGCAAATTCCCAAAGCTAATAACATGCAAGACACGTACGGTC
AAGAAGACATATTTGACCTCTTAACAGGTTCAGACGCGACTGCCTCATCAGTAAGACCCGTTGAAAAGAACTTACCTGAAAAAAACGAATATATACTAGCGTTGAAT
GTTAGCGTCAACAACAAGAAGTTTAATGACGCGGAGGCCAAGGCAAAAAGATTCCTTGATTACGTAAGGGAGTTAGAATCATTTTGAATAAAAAACACGCTTTTTCA
GTTCGAGTTTATCATTATCAATACTGCCATTTCAAAGAATACGTAAATAATTAATAGTAGTGATTTTCCTAACTTTATTTAGTCAAAAAATTAGCCTTTTAAAGCACGTG
TAACttGTAaATATCACGTGTAGGGGGCGGGTTACACAGAATATATAACATCGTAGGTaTCTaaGTGAACAGTTTATCACGTGCAaCgACTAAATATAATGGAGCCCGC
TTTTTAAGCTGtCATtCAGAAAAAAAAGAATCCCAGCACCAAAATATTGTTTTCTTCACCAACCATCAGTTCATAGGTCCATTCTCTTAGCGCAACTACAGAGAACAG
GGGCACAAACAGGCAAAAAACGGGCACAACCTCAATGGAGTGATGCAACCTGCCTGGAGTAAATGATGACACAAGGCAATTGACCCACGCATGTATCTATCTCATT
TTCTTACACCTTCTATTACCTTCTGCTCTCTCTGATTTGGAAAAAGCTGAAAAAAAAGGTTGAAACCAGTTCCCTGAAATTATTCCCCTACTTGACTAATAAGTATATAA
AGACGGTAGGTATTGATTGTAATTCTGTAAATCTATTTCTTAAACTTCTTAAATTCTACTTTTATAGTTAGTCTTTTTTTTAGTTTTAAAACACCAAGAACTTAGTTTCGA
ATAAACACACATAAACAAACAAAATG

D. Diagrams of the motif composition of the mutated promoter sequences. Cbf1p binding motifs are in red, Rap1p binding motifs in bronze, and Gcr1p binding motifs in gold. Mutations are indicated in lower case. The spacing between motifs from center to center is shown in base pairs. The PWM score for each wild-type motif is indicated beneath the motif. Diagrams are not to scale for the sake of nucleotide clarity.

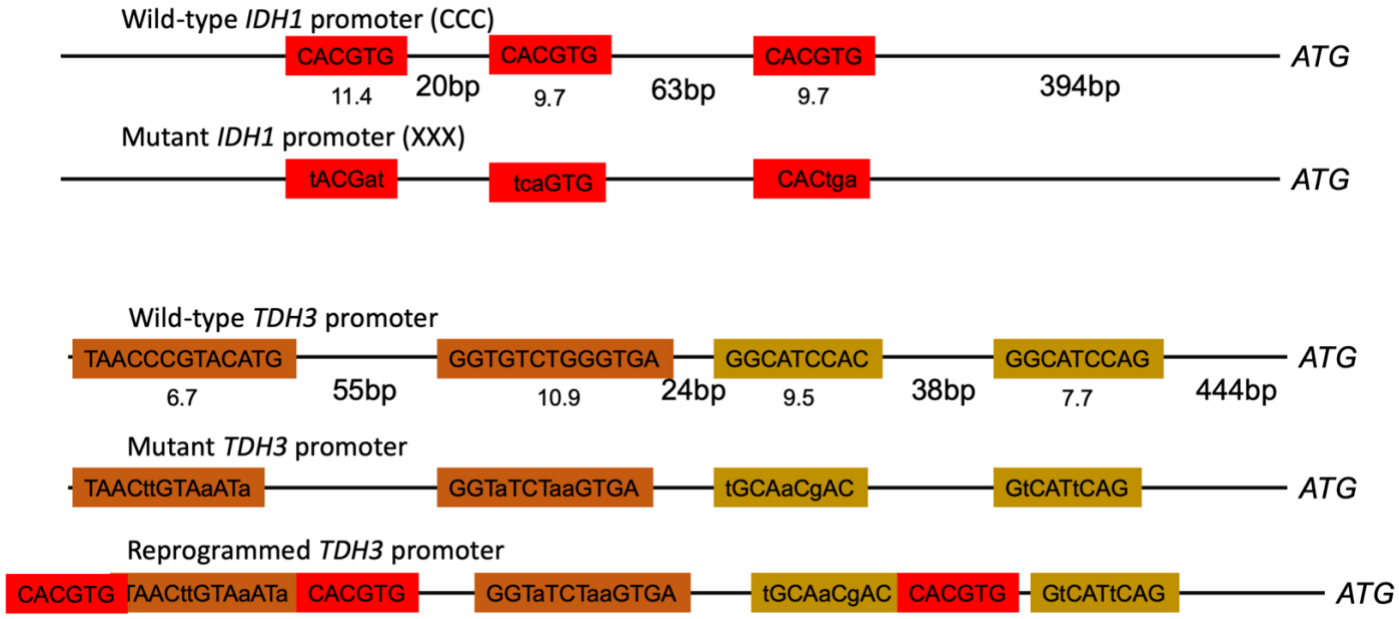

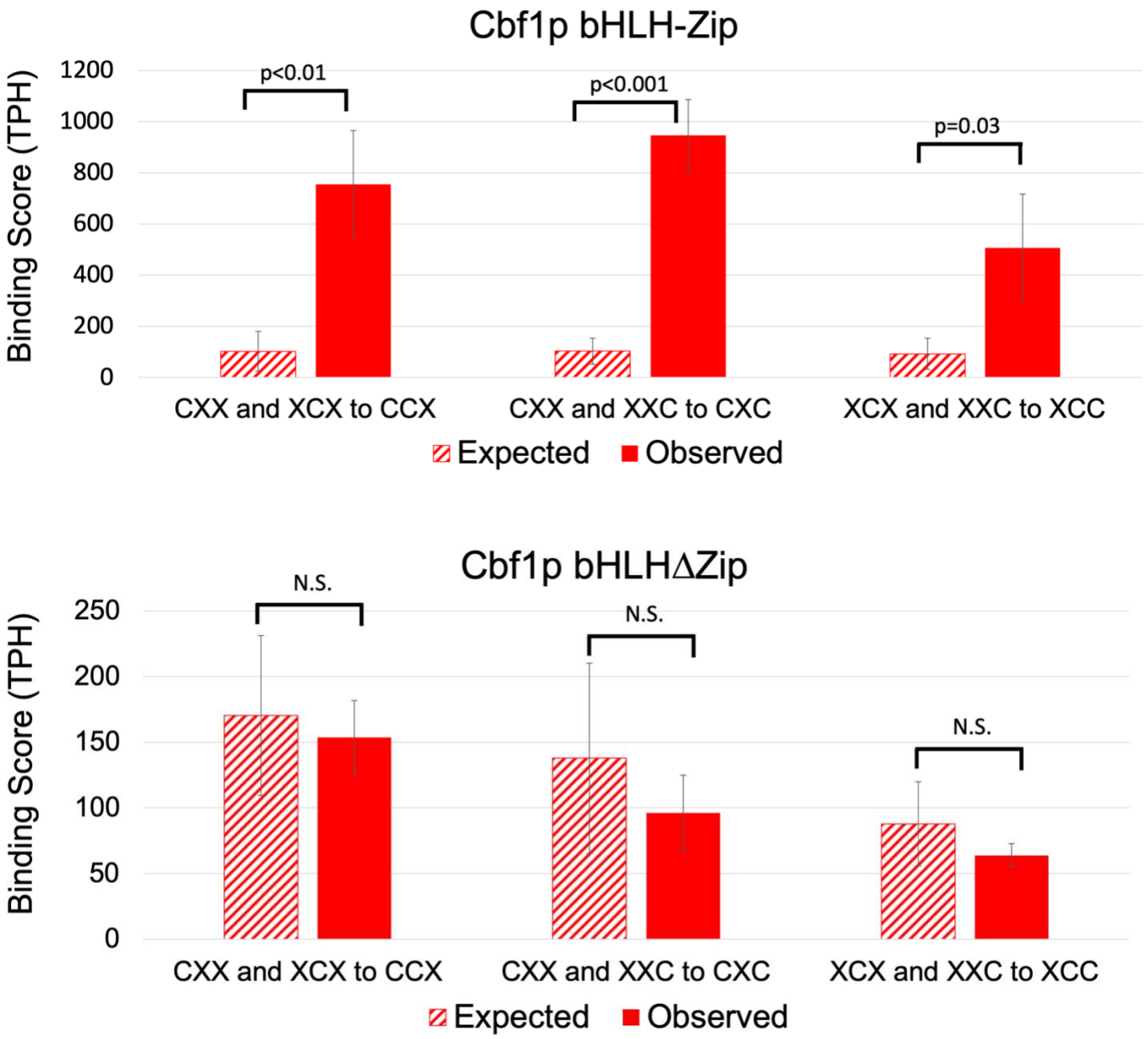

Fig. S9. Homotypic cooperativity of Cbf1p is observed at mutated *IDH1* promoters (the intergenic region between *IDH1* and *NCE103*) with 2 sites. If Cbf1p bHLH-Zip binds independently to its sites at the *IDH1* promoter, then the binding at *IDH1* promoter mutants with 2 intact sites should equal the sum of the Cbf1p bHLH-Zip binding scores measured at *IDH1* mutant promoters with the corresponding intact single sites. However, the binding of Cbf1p bHLH-Zip at mutant *IDH1* promoters with 2 Cbf1p motifs (solid bars, top panel) significantly exceeds the sum of the Cbf1p bHLH-Zip binding scores at the corresponding single site mutant promoters (checked bars, top panel), providing further evidence that Cbf1p bHLH-Zip binds with homotypic cooperativity. In contrast, Cbf1p bHLHΔZip binding at promoters with two Cbf1p sites (solid bars, bottom panel) is approximately equal to the sum of the Cbf1p bHLHΔZip binding scores at the corresponding single site mutant promoters (checked bars, bottom panel). Each bar in the plot represents the mean of 3 independent calling card assays and error bars indicate 1 standard deviation. The y-axis quantifies the observed and expected binding scores (TPH) and the exact motif configurations for each comparison is depicted under each pair of bars, with "X" representing a mutated motif and "C" representing an intact motif.

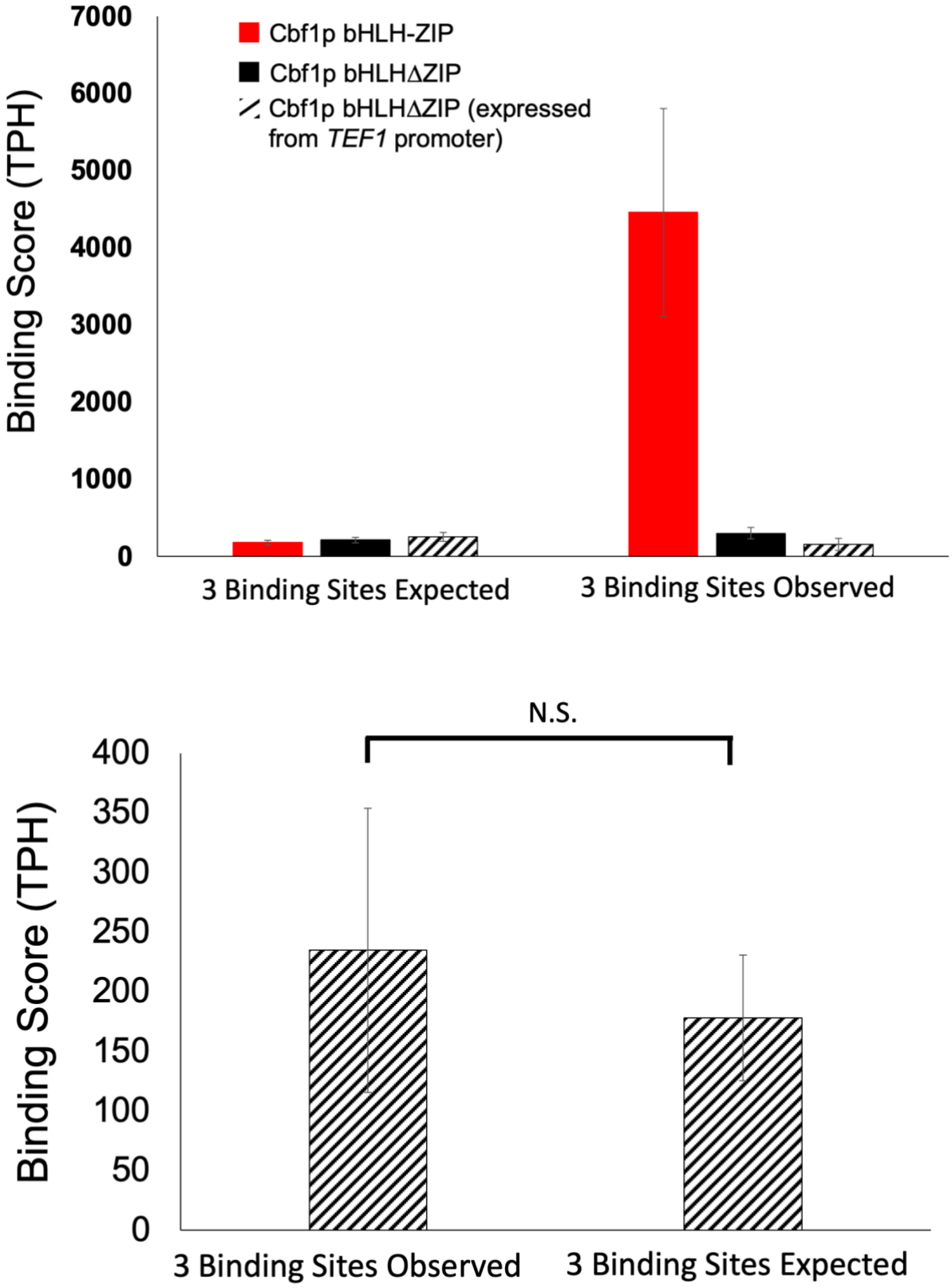

Fig. S10. The binding of Cbf1p bHLH-Zip, Cbf1p bHLHΔZip, and Cbf1p bHLHΔZip (expressed from the *TEF1* promoter) to mutated *IDH1* promoters with only one intact motif and the wild-type 3-motif promoter (the intergenic region between *IDH1* and *NCE103*) were assayed by calling cards in a *cbf1Δ met4Δ* strain (top). Cbf1p bHLHΔZip also does not display homotypic cooperative binding in a *cbf1Δ* (with a wild-type allele of *MET4*) strain when expressed from the *TEF1* promoter (bottom).

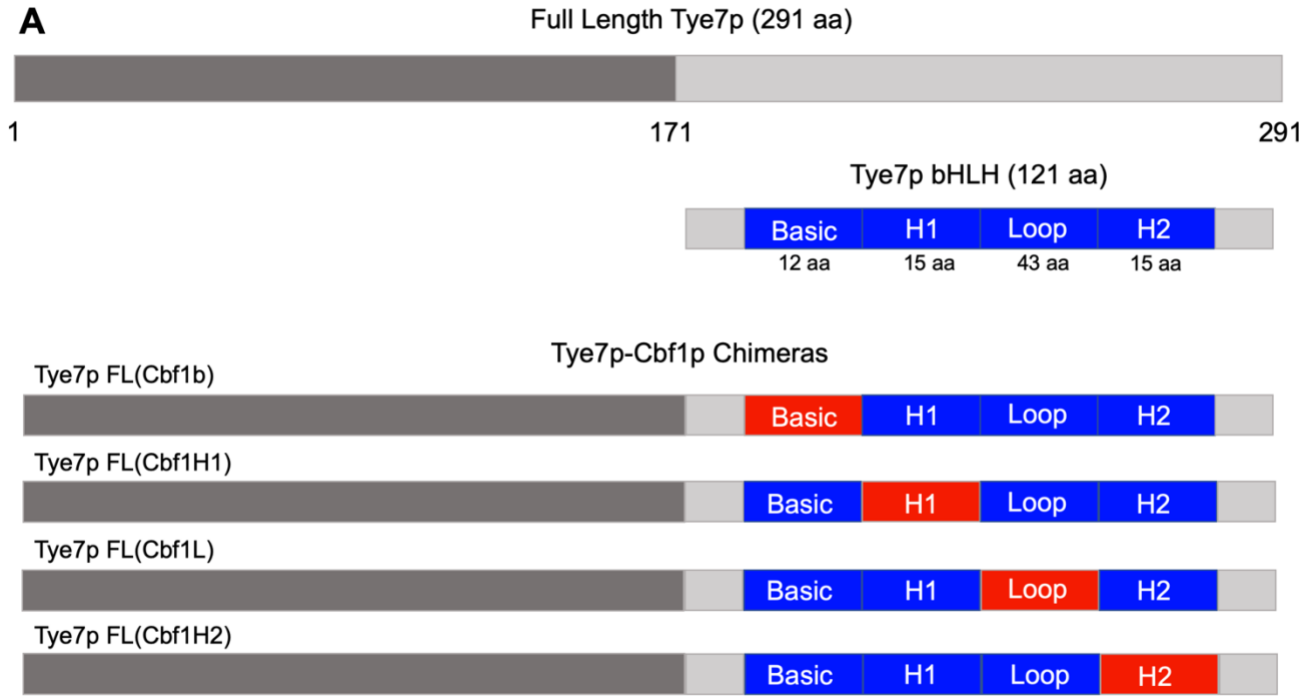
A
Full Length Tye7p (291 aa)
1
171
291
Tye7p bHLH (121 aa)
Basic
H1
Loop
H2
12 aa
15 aa
43 aa
15 aa
Tye7p-Cbf1p Chimeras
Tye7p FL(Cbf1b)
Tye7p FL(Cbf1H1)
Tye7p FL(Cbf1L)
Tye7p FL(Cbf1H2)

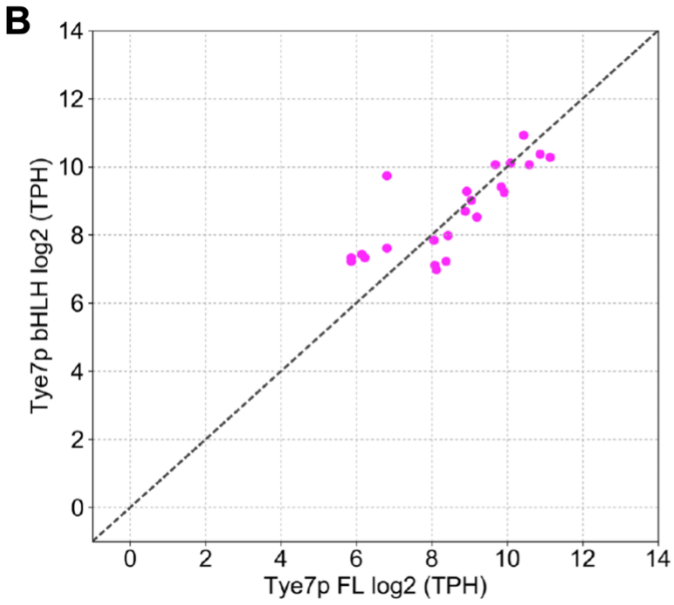
B
Tye7p bHLH log2 (TPH)
Tye7p FL log2 (TPH)
0
2
4
6
8
10
12
14

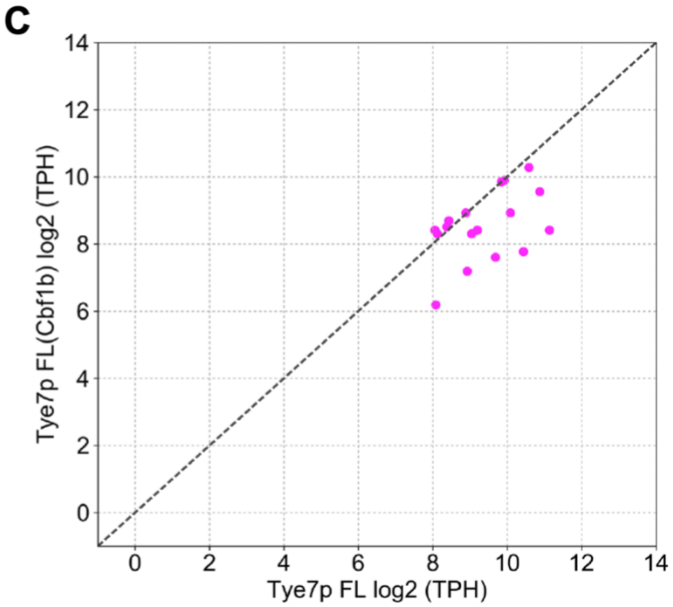
C
Tye7p FL(Cbf1b) log2 (TPH)
Tye7p FL log2 (TPH)
0
2
4
6
8
10
12
14

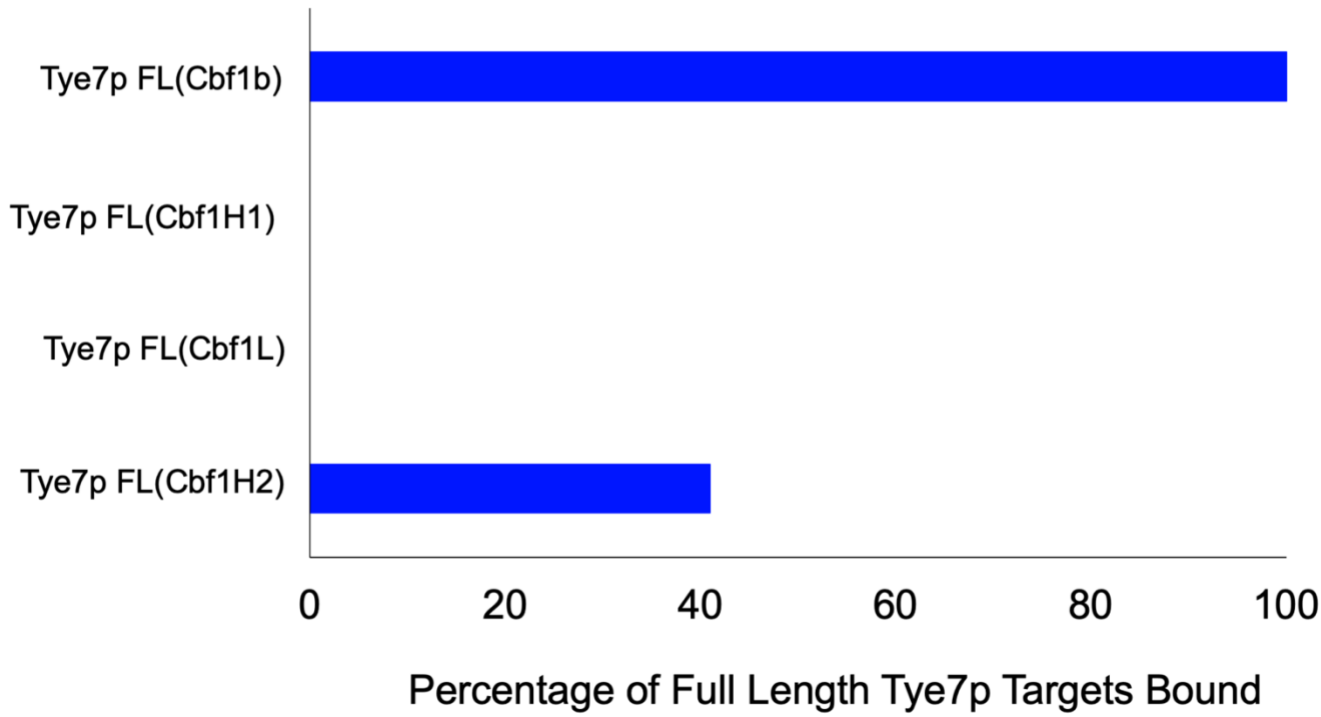

Fig. S11. A. Protein schematics of full-length, truncated, and chimeric Tye7p factors used in this study. Cbf1p bHLH sub-regions (red) that were switched with the homologous Tye7p sub-regions (blue). B. The Tye7p bHLH is sufficient to recapitulate the binding pattern of full-length (FL) Tye7p. The binding of Tye7p bHLH to each Tye7p-bound intergenic promoter region is plotted in $\log_2$ TPH. C. The genome-wide intergenic binding (TPH) of Tye7p FL vs. Tye7p FL(Cbf1p_b) is plotted, with each point representing a single intergenic region significantly bound by either factor. D. The percentage of Tye7p FL targets bound by each chimeric factor is indicated along the x-axis.

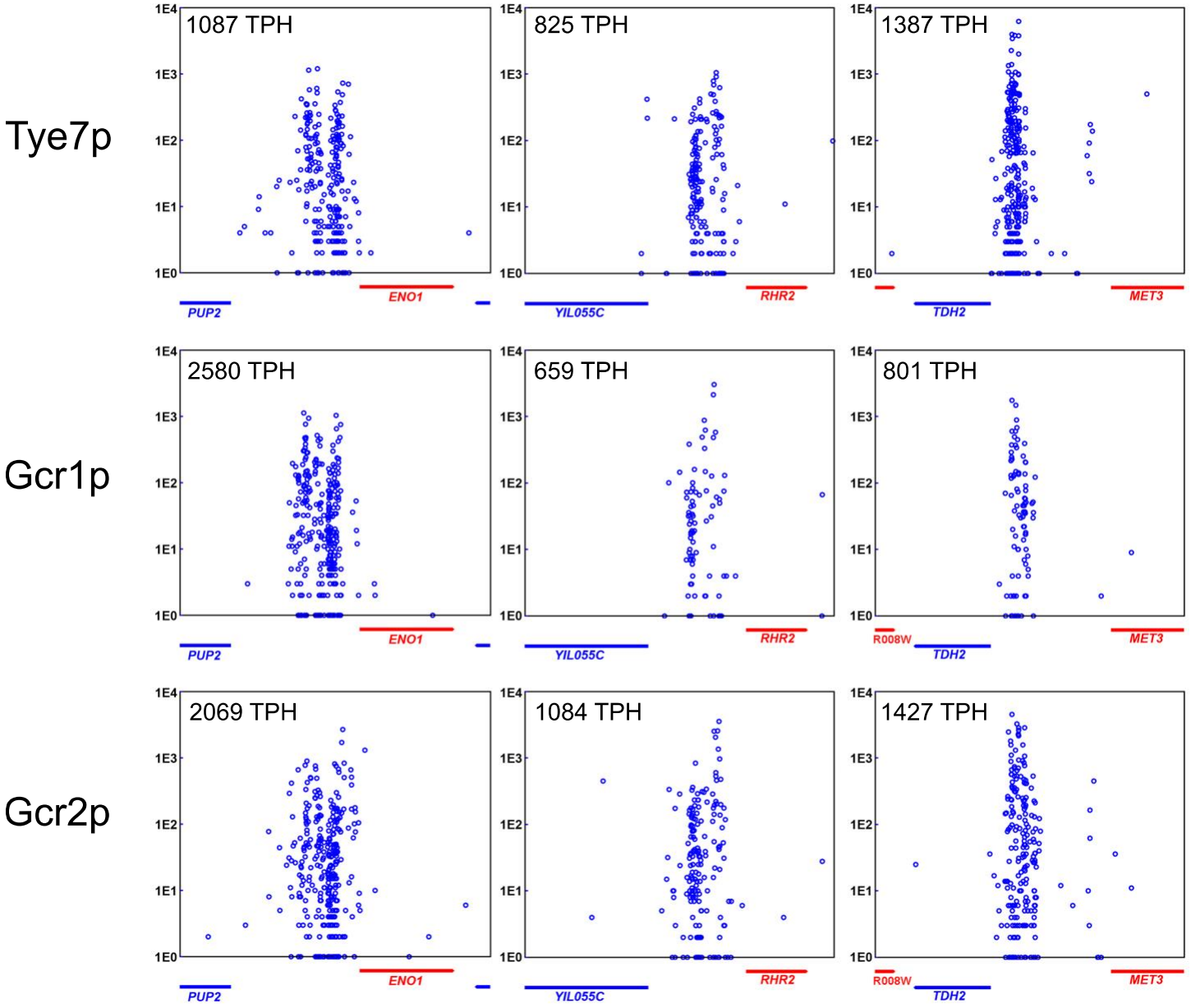

Fig. S12. Tye7p, Gcr1p, and Gcr2p co-occupy the same individual genomic loci. TF binding to *ENO1* (left), *RHR2* (middle), and *TDH2* (right) promoters.

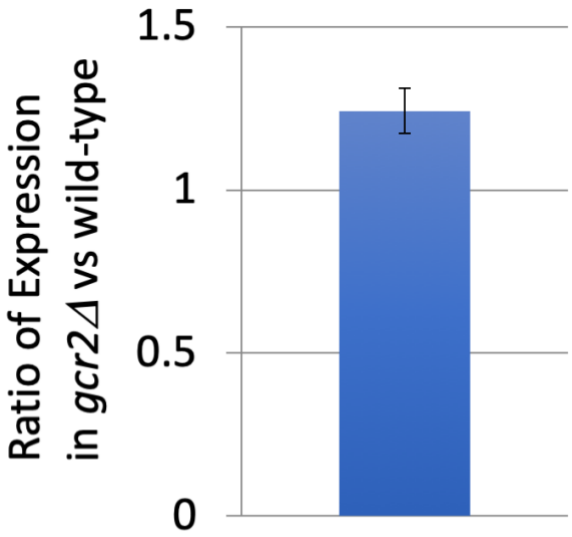

Fig. S13. The *TEF1* promoter is not regulated by *GCR2*. The average ratio of expression as measured by β-galactosidase assay from the *TEF1* promoter in *gcr2Δ* to wild-type is presented for 3 independent trials. Error bars indicate ± 1 standard deviation of 3 independent trials.

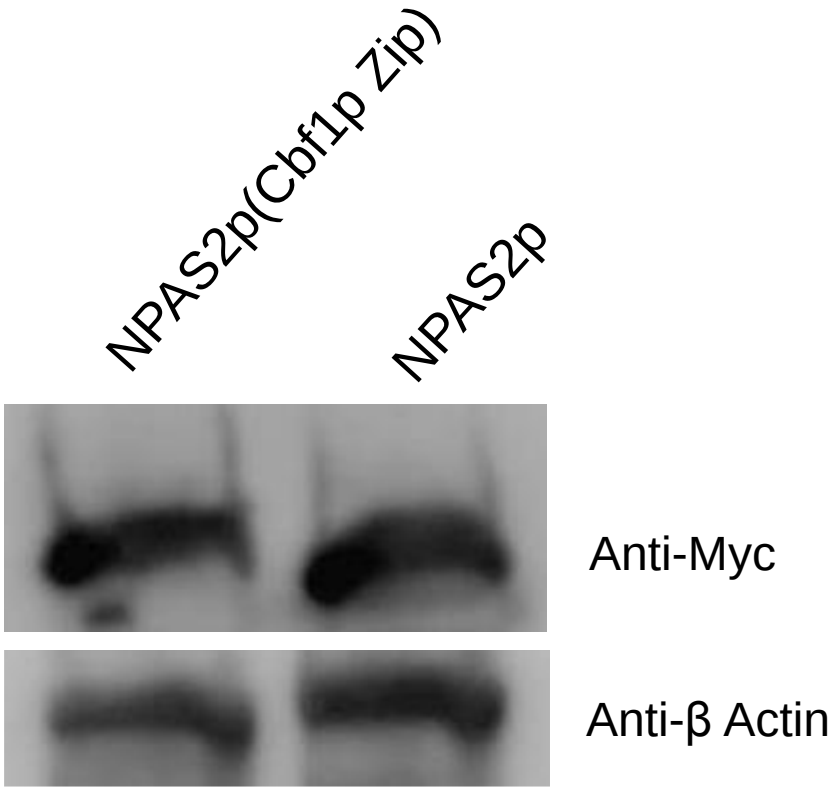

Fig. S14. NPAS2p and NPAS2p-(Cbf1p Zip) have equivalent expression in the *cbf1Δ met4Δ* strain. TFs were probed with antibody to the MYC tag, c-terminal to Sir4p, and probe against β-actin is shown as loading control.

TF (Binding Target Identification Method)	Significance of Tye7p Co-occupancy of Bound Intergenic Regions (p-value)
Sfp1p (ChIP-SEQ)	0.256
Sfp1p (Chec-SEQ)	0.065
Cst6p (Calling Cards)	0.0029*

Supplemental Table 1. Significance of Sfp1p and Cst6p co-occupancy with Tye7p at intergenic regions. The significance of overlap in Sfp1p (17) or Cst6p-bound and Tye7p-bound intergenic regions was determined by Fisher Exact test. *Co-occupancy of Cst6p and Tye7p-bound intergenic regions was found to be statistically though not biologically significant, as only 3 of Tye7p's 17 bound intergenic regions were also bound by Cst6p.

Intergenic Region	Left Feature	Right Feature	Left Common Name	Right Common Name	TPH	TPH Mutated *TDH3* pr	TPH Reprogrammed TDH3 pr
Chr7: 883815-884514	YGR192C	YGR193C	TDH3	PDX1	2254	35	41
Chr15: 160594-162356	YOL086C	YOL084W	ADH1	PHM7	1879	2159	2257
Chr2: 613895-616122	YBR196C	YBR198C	PGI1	TAF5	1537	1848	1550
Chr10: 454674-456232	YJR009C	YJR010W	TDH2	MET3	1387	829	1378
Chr7: 999145-1000932	YGR253C	YGR254W	PUP2	ENO1	1087	1571	1051
Chr5: 545050-545606	YER176W	YER177W	ECM32	BMH1	971	1122	1068
Chr13: 674765-677192	YMR205C	YMR207C	PFK2	HFA1	921	915	861
Chr9: 251911-255113	YIL056W	YIL053W	VHR1	RHR2	825	1295	1154
Chr8: 450806-451327	YHR172W	YHR174W	SPC97	ENO2	587	656	568
Chr12: 234082-235038	YLR044C	YLR045C	PDC1	STU2	529	794	534
Chr10: 337032-338266	YJL053W	YJL052W	PEP8	TDH1	487	984	482
Chr1: 69526-71787	YAL039C	YAL038W	CYC3	CDC19	475	432	276
Chr7: 973739-974880	YGR240C	YGR241C	PFK1	YAP1802	346	380	276
Chr11: 327131-327762	YKL060C	YKL059C	FBA1	MPE1	333	0	103
Chr16: 411282-412251	YPL076W	YPL075W	GPI2	GCR1	279	414	465
Chr15: 216137-217126	YOL060C	YOL059W	MAM3	GPD2	271	673	396
Chr11: 164390-166549	YKL152C	YKL150W	GPM1	MCR1	267	311	310

Supplemental Table 2. Binding scores at Tye7p target genes in a *TDH3* pr strain (wild-type), the mutated *TDH3* pr strain, and the reprogrammed *TDH3* pr strain.

Cooperative Binding Energy (KbT)	Pearson R (observed v. predicted)
0	0.35
-2	0.41
-4	0.53
-6	0.62
-8	0.69
-10	0.72

Supplemental Table 3. **Shea-Ackers Modeling of Cbf1p binding demonstrates a role for homotypic cooperativity.** To ascertain whether modeling the homotypic cooperativity more accurately predicts Cbf1p binding, we converted the PWM for Cbf1p to a free energy matrix following Heumann, Lapedes, and Stormo (18). We then implemented a Shea-Ackers thermodynamic model essentially as described by Segal and colleagues (19) to quantitatively predict the amount of Cbf1p binding at all Cbf1p bound intergenic regions with zero Cbf1p sites, one Cbf1p site, or multiple Cbf1p sites (within 500 bp of each other). To parameterize this model, Cbf1p nuclear concentration was estimated from Ghaemmaghami et al., (6890 molecules/nucleus, final nuclear concentration 1.14e-6 M) (20). Because the cooperativity between Cbf1p dimers depends strongly on the spacing and helical phasing between the sites (Jiayue Liu, manuscript in preparation), the value we measured at the *IDH1* promoter is not guaranteed to represent the average cooperativity per site. Therefore, we explored a number of different values for this cooperativity term, shown in the first column of Supplemental Table 3. This model shows that including any non-zero value of cooperativity (a negative free energy corresponds to positive cooperativity) is a better predictor of Cbf1p occupancy than if no cooperativity is assumed. These data show that cooperativity is necessary to accurately describe the genome-wide binding of Cbf1p. Code and a Jupyter Notebook describing these results are available at https://gitlab.com/rob.mitra/shively_2019.

Saccharomyces cerevisiae strain	Genotype	Reference
BY4741	*MATa his3Δ1 leu2Δ0 met15Δ0 ura3Δ0*	(1)
BY4742	*MATα his3Δ1 leu2Δ0 lys2Δ0 ura3Δ0*	(1)
yRM1070	*MATa his3Δ1 leu2Δ0 met15Δ0 ura3Δ0 sir4Δ::hphMX4*	This Study
yRM1072	*MATα his3Δ1 leu2Δ0 lys2Δ0 ura3Δ0 sir4Δ::hphMX4*	This Study
yRM1073	*MATa his3Δ1 leu2Δ0 met15Δ0 ura3Δ0 sir4Δ::hphMX4 cbf1Δ::kanMX4*	This Study
yRM1074	*MATα his3Δ1 leu2Δ0 lys2Δ0 ura3Δ0 sir4Δ::hphMX4 cbf1Δ::kanMX4 opi1Δ::URA3 met4Δ::natMX4*	This Study
yRM1075	*MATα his3Δ1 leu2Δ0 lys2Δ0 ura3Δ0 sir4Δ::hphMX4 cbf1Δ::kanMX4*	This Study
yRM1076	*MATa his3Δ1 leu2Δ0 met15Δ0 ura3Δ0 CBF1-SIR4::natMX4 sir4Δ::hphMX4*	This Study
yRM1077	*MATa his3Δ1 leu2Δ0 met15Δ0 ura3Δ0 TYE7-SIR4::natMX4 sir4Δ::kanMX4 trp1Δ::hphMX4*	This Study
yRM1078	*MATa his3Δ1 leu2Δ0 met15Δ0 ura3Δ0 sir4Δ::hphMX4 gcr2Δ::kanMX4*	This Study
yRM1079	*MATa his3Δ1 leu2Δ0 met15Δ0 ura3Δ0 sir4Δ::hphMX4 pTDH3-1* (*TDH3* promoter has been mutated to remove Gcr1/2p and Rap1p sites and add Cbf1p sites)	This Study
yRM1080	*MATa his3Δ1 leu2Δ0 met15Δ0 ura3Δ0 sir4Δ::hphMX4 cbf1Δ::kanMX4 pIDH1-1* (CCX configuration of Cbf1p sites)	This Study
yRM1081	*MATa his3Δ1 leu2Δ0 met15Δ0 ura3Δ0 sir4Δ::hphMX4 cbf1Δ::kanMX4 pIDH1-2* (CXX configuration of Cbf1p sites)	This Study
yRM1082	*MATa his3Δ1 leu2Δ0 met15Δ0 ura3Δ0 sir4Δ::hphMX4 cbf1Δ::kanMX4 pIDH1-3* (CXC configuration of Cbf1p sites)	This Study
yRM1083	*MATa his3Δ1 leu2Δ0 met15Δ0 ura3Δ0 sir4Δ::hphMX4 cbf1Δ::kanMX4 pIDH1-4* (XCC configuration of Cbf1p sites)	This Study
yRM1084	*MATa his3Δ1 leu2Δ0 met15Δ0 ura3Δ0 sir4Δ::hphMX4 cbf1Δ::kanMX4 pIDH1-5* (XCX configuration of Cbf1p sites)	This Study
yRM1085	*MATa his3Δ1 leu2Δ0 met15Δ0 ura3Δ0 sir4Δ::hphMX4 cbf1Δ::kanMX4 pIDH1-6* (XXC configuration of Cbf1p sites)	This Study
yRM1086	*MATa his3Δ1 leu2Δ0 met15Δ0 ura3Δ0 sir4Δ::hphMX4 cbf1Δ::kanMX4 pIDH1-7* (XXX configuration of Cbf1p sites)	This Study
yRM1087	*MATa his3Δ1 leu2Δ0 met15Δ0 ura3Δ0 sir4Δ::hphMX4 pTDH3-2* (*TDH3* promoter has been mutated to remove Rap1p and Gcr1/2p binding sites)	This Study

Supplemental Table 4. Yeast strains used in this study.

SI References

1. Brachmann CB, et al. (1998) Designer deletion strains derived from Saccharomyces cerevisiae S288C: a useful set of strains and plasmids for PCR-mediated gene disruption and other applications. *Yeast Chichester Engl* 14(2):115–132.

2. Hickman MJ, et al. (2011) Coordinated regulation of sulfur and phospholipid metabolism reflects the importance of methylation in the growth of yeast. *Mol Biol Cell* 22(21):4192–4204.

3. Boeke JD, Trueheart J, Natsoulis G, Fink GR (1987) 5-Fluoroorotic acid as a selective agent in yeast molecular genetics. *Methods Enzymol* 154:164–175.

4. Rothstein R (1991) Targeting, disruption, replacement, and allele rescue: integrative DNA transformation in yeast. *Methods Enzymol* 194:281–301.

5. Wang H, Heinz ME, Crosby SD, Johnston M, Mitra RD (2008) "Calling Cards" method for high-throughput identification of targets of yeast DNA-binding proteins. *Nat Protoc* 3(10):1569–1577.

6. Wang H, Mayhew D, Chen X, Johnston M, Mitra RD (2011) Calling Cards enable multiplexed identification of the genomic targets of DNA-binding proteins. *Genome Res* 21(5):748–755.

7. Sievers F, et al. (2011) Fast, scalable generation of high-quality protein multiple sequence alignments using Clustal Omega. *Mol Syst Biol* 7:539.

8. Wang H, Johnston M, Mitra RD (2007) Calling cards for DNA-binding proteins. *Genome Res* 17(8):1202–1209.

9. Spivak AT, Stormo GD (2012) ScerTF: a comprehensive database of benchmarked position weight matrices for Saccharomyces species. *Nucleic Acids Res* 40(Database issue):D162-168.

10. Heinz S, et al. (2010) Simple combinations of lineage-determining transcription factors prime cis-regulatory elements required for macrophage and B cell identities. *Mol Cell* 38(4):576–589.

11. Harbison CT, et al. (2004) Transcriptional regulatory code of a eukaryotic genome. *Nature* 431(7004):99–104.

12. Korhonen J, Martinmäki P, Pizzi C, Rastas P, Ukkonen E (2009) MOODS: fast search for position weight matrix matches in DNA sequences. *Bioinforma Oxf Engl* 25(23):3181–3182.

13. Pizzi C, Rastas P, Ukkonen E (2011) Finding significant matches of position weight matrices in linear time. *IEEE/ACM Trans Comput Biol Bioinform* 8(1):69–79.

14. Gitter A, et al. (2009) Backup in gene regulatory networks explains differences between binding and knockout results. *Mol Syst Biol* 5:276.

15. Zentner GE, Kasinathan S, Xin B, Rohs R, Henikoff S (2015) ChEC-seq kinetics discriminates transcription factor binding sites by DNA sequence and shape in vivo. *Nat Commun* 6:8733.

16. Kang Y, et al. (2019) Mapping Transcription Factor Networks By Comparing Tf Binding Locations To Tf Perturbation Responses. *bioRxiv*. doi:10.1101/619676.

17. Albert B, et al. (2019) Sfp1 regulates transcriptional networks driving cell growth and division through multiple promoter-binding modes. *Genes Dev* 33(5–6):288–293.

18. Heumann JM, Lapedes AS, Stormo GD (1994) Neural networks for determining protein specificity and multiple alignment of binding sites. *Proc Int Conf Intell Syst Mol Biol* 2:188–194.

19. Raveh-Sadka T, Levo M, Segal E (2009) Incorporating nucleosomes into thermodynamic models of transcription regulation. *Genome Res* 19(8):1480–1496.

20. Ghaemmaghami S, et al. (2003) Global analysis of protein expression in yeast. *Nature* 425(6959):737–741.